Work Functions and Surface Functional Groups of Multiwall Carbon Nanotubes

Hiroki Ago,*,†,‡ Thomas Kugler,§ Franco Cacialli,† William R. Salaneck,§ Milo S. P. Shaffer,|| Alan H. Windle,|| and Richard H. Friend†

Cavendish Laboratory, University of Cambridge, Madingley Road, Cambridge, CB3 0HE, U.K., Department of Molecular Engineering, Graduate School of Engineering, Kyoto University, Sakyo-ku, Kyoto 606-8501, Japan, Department of Physics and Measurement Technology, Linköping University, S-581 83, Linköping, Sweden, and Department of Materials Science and Metallurgy, University of Cambridge, Pembroke Street, Cambridge, CB2 3QZ, U.K.

Received: May 19, 1999; In Final Form: July 29, 1999

We have studied the work function and density of states (DOS) of multiwall carbon nanotubes (MWNTs) using ultraviolet photoelectron spectroscopy (UPS). Raw MWNTs were purified by successive sonication, centrifugation, sedimentation, and filtration processes with the aid of a nonionic surfactant. The purified MWNTs showed a slightly lower work function (4.3 eV) than that of highly oriented pyrolytic graphite (4.4 eV). Effects of three different oxidative treatments, air-, oxygen plasma-, and acid-oxidation, have also been studied. It was found that oxidative treatments affect the DOS of valence bands and increase the work function. X-ray photoelectron spectroscopy (XPS) measurements have suggested that gas-phase treatment preferentially forms hydroxyl and carbonyl groups, while liquid-phase treatment forms carboxylic acid groups on the surface of MWNTs. These surface chemical groups disrupt the π-conjugation and introduce surface dipole moments, leading to higher work functions up to 5.1 eV. We expect the information on the work function of the MWNTs to be of importance to the development of electronic or optoelectronic applications.

I. Introduction

Carbon nanotubes have attracted increased interest because of their peculiar one-dimensional structure, consisting of rolled up graphene sheets with a nanoscale diameter and a variety of electronic structures.[1,2] Quantum chemical calculations have predicted that the electronic structure of a carbon nanotube changes from metallic to semiconducting depending on the chiral angle of the atomic lattice and the diameter.[3−6] Experimentally, scanning tunneling spectroscopy (STS) studies of several single-wall carbon nanotubes (SWNTs) have shown that SWNTs with certain atomic configurations possess a finite electronic density of states (DOS) at the Fermi energy, while others have no DOS.[7,8] These two types of SWNTs are interpreted as metallic and semiconducting SWNTs, respectively.

In addition to these fundamental issues, carbon nanotubes are expected to find wide applications as a result of their stability, mechanical strength, and characteristic structure. Multiwall carbon nanotubes (MWNTs) are more frequently studied than SWNTs because of the stability and the relative ease of surface modification while maintaining high conductivity. The interface between nanotubes and a metal or a semiconductor becomes very important if nanotubes are to be employed in electronic devices.[7] One of the most important factors that determines the interaction at the interface is the relative values of the work functions. Work functions are essential for designing nanotube-based macroscale devices, such as diodes,[9] light-emitting diodes,[10] and photovoltaic devices.[11] However, as yet, reliable work functions of carbon nanotubes have not been obtained and, hence, have been assumed to be the same as that of graphite. We note that although work function can be estimated from field-emission spectra using a Fowler−Nordheim model, the resulting values are not reliable because of uncertainty in the parameters employed and the nonlinear behavior of the spectra. In fact a wide range of work functions from 0 to 8 eV have been reported.[12−14]

Since carbon nanotubes are insoluble and difficult to handle, oxidative treatments have been frequently used for many purposes, such as purification,[15,16] as a stage in chemical modification,[17] in order to disperse in solvents,[18] and for improvement of field emission.[19] Despite these developments, however, little is known about the effects of oxidation on the electronic structure. From the viewpoint of the surface chemistry of carbon nanotubes, it is also important to investigate systematically the functional groups introduced by these reactions.

In this paper, we report on ultraviolet photoelectron spectroscopy (UPS) and X-ray photoelectron spectroscopy (XPS) results for MWNTs. UPS is a powerful technique for the investigation of both the valence band DOS and the work function. XPS yields information on surface chemical groups. Two main difficulties, film preparation and charging effects, were resolved by filtering MWNTs dispersion onto filter membranes precoated with indium−tin oxide (ITO). We chose ITO as a metallic contact because ITO possesses a very low DOS at the energy range studied, being different from other metals such as gold. We also report the effects of three different oxidative treatments (air-, oxygen plasma-, and acid-oxidation) on the electronic structure and the surface chemical groups.

* Present address: National Institute of Materials and Chemical Research (NIMC), Tsukuba, 305-8565, Japan. E-mail: ago@nimc.go.jp.
† Cavendish Laboratory, University of Cambridge.
‡ Kyoto University.
§ Linköping University.
|| Department of Materials Science and Metallurgy, University of Cambridge.

10.1021/jp991659y CCC: $18.00
Published on Web 09/03/1999

II. Experimental Section

The following four types of MWNTs and, for comparison, a cleaved surface of highly oriented pyrolytic graphite (HOPG) were studied for UPS and XPS measurements.

(i) Purified MWNTs. Raw MWNTs prepared by arc-evaporation method (Vacuum Metallurgical Co. Ltd.) were dispersed in distilled water with 5 wt. % of a nonionic surfactant, t-octylphenoxypolyethoxyethanol (TRITON X-100). It is noted that MWNTs are free from metallic catalysts which may affect UPS spectra. Purification was based on methods described in the literature:[20] large graphitic particles were removed by repeated sonication, centrifugation, and sedimentation processes, while the nanoparticles were removed by filtration onto ITO-precoated polycarbonate filter membranes with 1.0 μm pores (Whatman Cyclopore). After the filtration, the film was washed with distilled water to remove the surfactant.

(ii) Air-Oxidized MWNTs. The raw arc-evaporated MWNTs were oxidized in air flow at around 900 °C for 15 min. The remaining MWNTs (about 1 wt. %) were purified by the same procedure employed for (i).

(iii) Plasma-Oxidized MWNTs. A purified arc-evaporated MWNT film (i) was subjected to oxygen plasma treatment with applied power of 400 W for 15 min.

(iv) Acid-Oxidized MWNTs. Catalytically grown MWNTs were employed because it has been shown that acid-oxidized catalytically grown MWNTs realize highly concentrated dispersions without surfactants, which in turn can be very useful for further processing.[11,18] The raw MWNTs were oxidized in a mixed solution of HNO_3 and H_2SO_4 at 130 °C for 1 h, followed by filtering onto a glass filter and washing with distilled water. This acid-oxidation removed the metal catalyst used for the synthesis of the MWNTs. Since the catalytically grown MWNTs used were essentially free from carbon impurities, no further purification was performed. Finally, acid-oxidized MWNTs were dispersed in water again and filtered onto the ITO-coated filter membranes.

UPS and XPS measurements were performed in ultrahigh vacuum (UHV) ($<10^{-10}$ Torr). Sample surfaces were cleaned by heat treatment at 100 °C in UHV prior to the measurements. UPS spectra were obtained using irradiation of HeII 40.8 eV ultraviolet light. Work functions were determined from the secondary electron cutoff of UPS HeI spectra using gold metal (5.1 eV) as a reference. XPS spectra were measured using a MgKα (1235.6 eV) line. Owing to the ITO coating, charging effects during the measurements were successfully avoided. The thickness of the ITO (340 nm) was sufficient to ensure that the effects of the polycarbonate filter on the C_{1s} XPS could be neglected. We have also examined the materials using scanning electron microscopy (SEM) and transmission electron microscopy (TEM) using a JEOL JSM-6340F and a JEOL 2000EX, respectively.

III. Results and Discussion

1. Purified MWNT. Figure 1 shows a SEM image of a purified MWNT film. It can be seen that the purification procedure removed the large graphitic particles and that a surfactant untangled the bundles of MWNTs. Inhomogeneity of the MWNT film is due the localized influence of the micropores. A TEM micrograph of a purified MWNT is shown in Figure 2(a). Purified MWNTs were straight with closed tips, as is typical of arc-evaporated MWNTs. It was found that their outer surfaces are partially covered with a surfactant even after washing with water. This fact suggests that there should be a contribution from the surfactant to the photoelectron spectroscopy results. It should be noted that XPS spectra are less affected by the presence of the surfactant, compared with UPS spectra, because of the difference in detectable depth (UPS and XPS techniques probe depth of up to 1 and 5 nm from the surface, respectively).

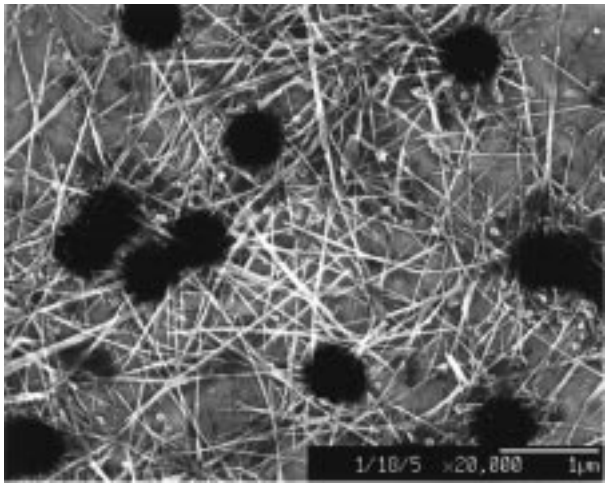

Figure 1. SEM picture of a purified MWNT film prepared by filtration of a MWNT−water dispersion onto an ITO-coated polycarbonate filter membrane. Black circles correspond to pores of the filter membrane.

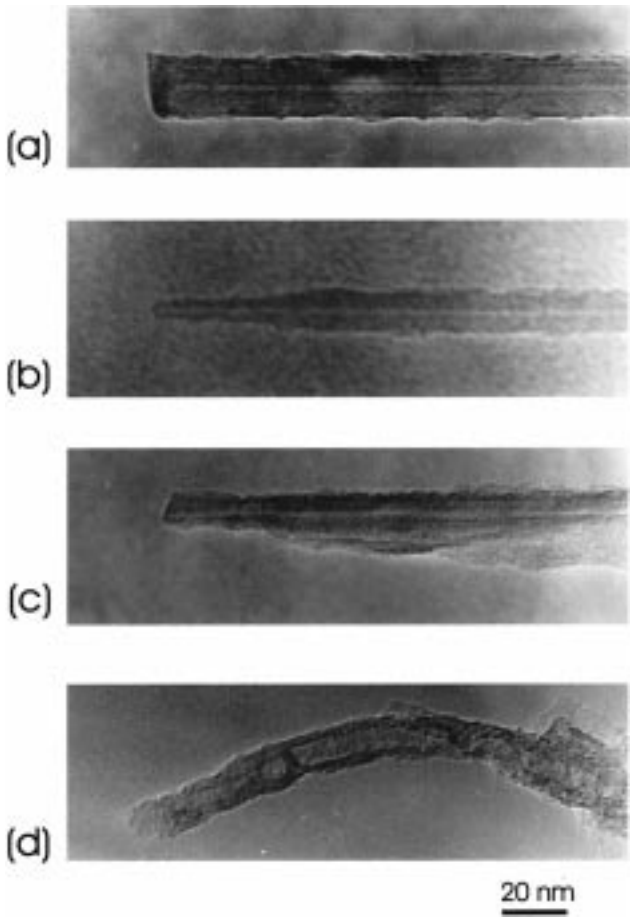

Figure 2. TEM images of tips of (a) purified, (b) air-, (c) plasma-, and (d) acid-oxidized MWNTs.

The work functions determined from HeI spectra are listed in Table 1. The purified MWNTs had a work function of 4.3 eV. This value is slightly lower than that of graphite (4.4 eV). As described below (see section 2.1), even the purified MWNTs suffered oxidation during the purification process, with subse-

TABLE 1: Work Functions of MWNTs and Graphite Determined from the Cutoff of the Secondary Electron in UPS HeI Spectra

sample	work function (eV)
purified MWNTs	4.3
air-oxidized MWNTs	4.4
plasma-oxidized MWNTs	4.8
acid-oxidized MWNTs	5.1
highly oriented pyrolytic graphite (HOPG)	4.4

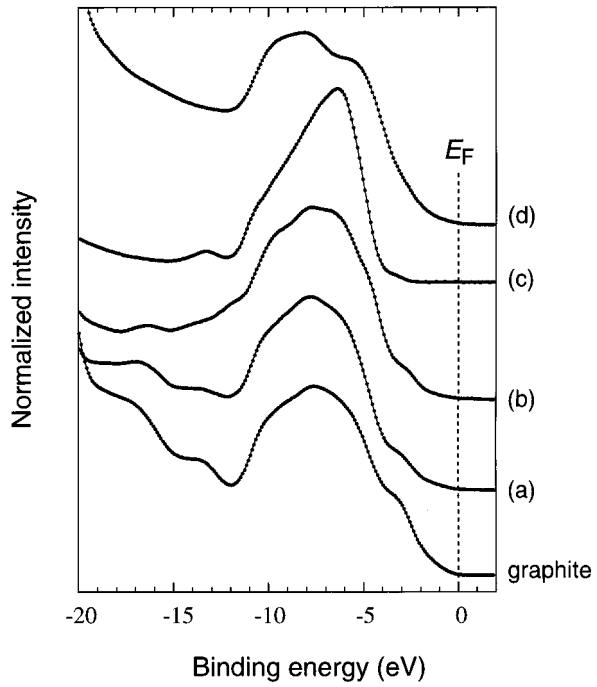

Figure 3. UPS spectra of graphite and (a) purified, (b) air-, (c) plasma-, and (d)acid-oxidized MWNTs. E_F denotes the Fermi level of the materials.

quent increase of the work function; the lower work function of the MWNTs compared to graphite is therefore considered to represent an intrinsic property.[21] In other words, the binding energy of π-electrons is smaller for MWNTs than for graphite. This lower work function of MWNTs could be explained in terms of destabilization of the π-electrons due to curvature of the graphene sheets. The electron emission from the tips of MWNTs is unlikely in the present case because the MWNTs lie almost parallel to the filter surface. To the best of our knowledge, there has been no theoretical investigation of this work function difference. From the above result, we speculate that highly efficient field emission from MWNTs is not originated in their very low work functions (0−2 eV)[13,14] but in their specific one-dimensional structure.

In Figure 3, we report the UPS spectra corresponding to valence band DOS. A peak at −3 eV originates in the valence bands with pπ-nature, while the main peak at −8 eV stems from valence bands with pσ-nature.[22] It can be seen that a UPS spectrum of purified MWNTs resembles that of graphite, reflecting the similarity of their electronic structures. This similarity has also been suggested by electron-energy loss spectroscopy (EELS) measurements.[23] It is seen that the relative intensity of the pπ-derived DOS to the pσ-derived DOS is smaller for the MWNTs than that of graphite. This can be accounted for by the presence of defect sites and the residual surfactant of the purified MWNTs, as identified in the C_{1s} XPS spectrum described below.

It is worthwhile to compare the work functions of purified SWNTs and MWNTs. Our preliminary measurements of SWNTs purified by acid-oxidation in Rice group showed the work function of 4.8 eV.[24] At the moment we cannot simply compare the purified SWNTs and MWNTs because of the chemical oxidation applied to the SWNTs. The result will be reported elsewhere.[24]

2. Effects of Oxidative Treatments. *2.1. Geometrical and Electronic Structure.* In this section, we will consider the effects of three kinds of oxidative treatments. As displayed in Figure 2(b−d), the structures of the MWNTs are found to be strongly modified by oxidative treatments. In the case of air-oxidation, we observed that the oxidation proceeds mainly from the tips, leading to opening and subsequent thinning of the MWNTs from the ends.[25] In addition, swelling of the outer layers was also observed. The oxidation proceeds inhomogeneously, and some part of the surface of the MWNTs remained unreacted. Plasma-oxidation caused severe damage to the MWNTs, forming a very rough surface (Figure 2(c)). Acid-oxidized MWNTs had a different structure than arc-evaporated MWNTs because they were prepared by a different catalytic method. The raw catalytically grown MWNTs already contain a number of defects and, thus, are not straight. It has been reported that defects in catalytically grown MWNTs enhance the oxidation which proceeds at sites along full length of the MWNTs.[18]

In addition to these structural changes, we have observed different work functions for oxidized MWNTs. We found that the work functions of all oxidized MWNTs are higher than that of purified MWNTs and that the absolute value is strongly dependent on the treatment (Table 1). Air-oxidized MWNTs showed only a slight increase in their work function, while plasma- and acid-oxidized MWNTs showed much higher work functions. The increase in work function can be explained by the following two mechanisms: (i) a reduction of the π-conjugation of the MWNTs, which reduces the pπ-derived DOS and (ii) an enhancement of the surface dipoles pointing inward because of the presence of oxygen-containing functional groups. On the basis of these mechanisms, the higher work functions of plasma- and acid-oxidized MWNTs relative to that of air-oxidized MWNTs are in accordance with the observed structures under the TEM (Figure 2). An illustration of the spatial energy diagram of an oxidized MWNT is shown in Figure 4. We speculate that the work function at the core of a MWNT (ϕ_{pure}) is not higher than 4.3 eV assuming that the inner graphene layers remain unreacted. The oxidized outer layers (ϕ_{oxi}) are considered to have higher work functions for the reasons given above.

As well as the work functions, both pπ- and pσ-derived DOS were found to be significantly affected by oxidative treatment as shown in Figure 3. Air-oxidation is relatively mild and induced only a slight increase in the pσ-derived DOS at −6 eV. From a comparison with purified MWNTs, one can also see that the pπ-derived DOS became slightly smaller, reflecting reduction in π-conjugation of the outer surfaces of MWNTs. The origin of the increase in the DOS at −6 eV and −12 eV is unclear but might be assigned to H_2O or nitrogen atoms incorporated during air-oxidation, on the basis of results reported for amorphous carbons.[26,27] In contrast to air-oxidation, we found that plasma-oxidation causes a drastic change in the electronic structure. The pπ-derived DOS is significantly reduced and even the main pσ-DOS was strongly affected. We consider that the main reason for this change was the transformation of the graphene layers to amorphous carbon phase with an sp^3 network, as revealed by XPS and discussed below. Acid-oxidation, on the other hand, reduced the pπ-derived DOS at −3 eV and increased the pσ-derived DOS at −5.6 and −9.8 eV. Note that

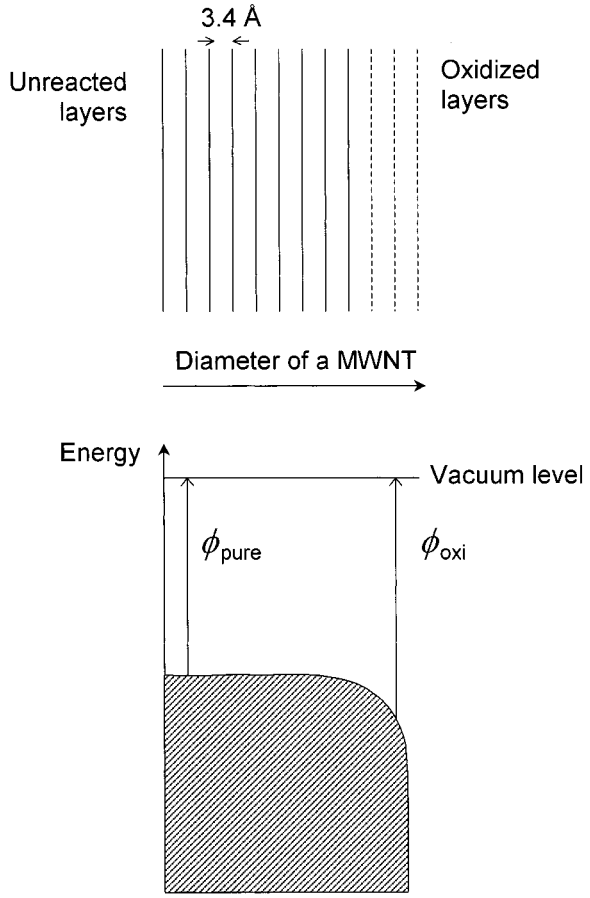

Figure 4. Illustration of the spatial distribution of the work function of a MWNT. Upper shows a cross-section of an oxidized MWNT, where solid and broken lines indicate unreacted and oxidized graphene layers. Note that in the actual MWNTs the whole surface area is not fully oxidized as in the illustration. Lower shows the corresponding valence band of the MWNT. The notations, ϕ_{pure} and ϕ_{oxi}, indicate work functions at each position.

these DOS features also differ from the MWNTs oxidized by the other treatments.

2.2. Surface Functional Groups. In this last section, we discuss the chemical species introduced by oxidative treatment, as determined from XPS results. In Figure 5 we show the C1s XPS spectrum of a basal plane of highly oriented pyrolytic graphite. As is well known, graphite shows an asymmetric peak centered at 284.66 eV with a long tail extended to the higher energy region.[28] This peak feature has been explained in terms of many-electron interactions of the metallic conduction electrons induced by low energy electron−hole excitations resulting from the absorption of X-rays.

The asymmetric peak was observed for all the MWNT films (Figure 5(a−d)), centered at 284.5 ± 0.1 eV. We have performed a deconvolution of the C_{1s} spectrum of MWNTs into an asymmetric peak of graphite (284.5 ± 0.2 eV) and four Gaussian peaks centered at 285.1 ± 0.2, 286.2 ± 0.2, 287.5 ± 0.2, and 288.9 ± 0.2 eV. The main peak at 284.5 eV originates in both sp^2-hybryidized graphite-like carbon atoms and in carbon atoms bound to hydrogen atoms. A peak at 285.1 eV can be assigned to sp^3-hybridized carbon atoms as in diamond-like carbon. We note that these two peaks are observed in amorphous carbons and that their relative intensity correlates with the degree of graphitization.[29] Peaks with higher binding energies located at 286.2, 287.5, and 288.9 eV are considered to originate in carbon atoms bound to one, two, and three oxygen atoms, respectively, because electronegative oxygen atoms induce a

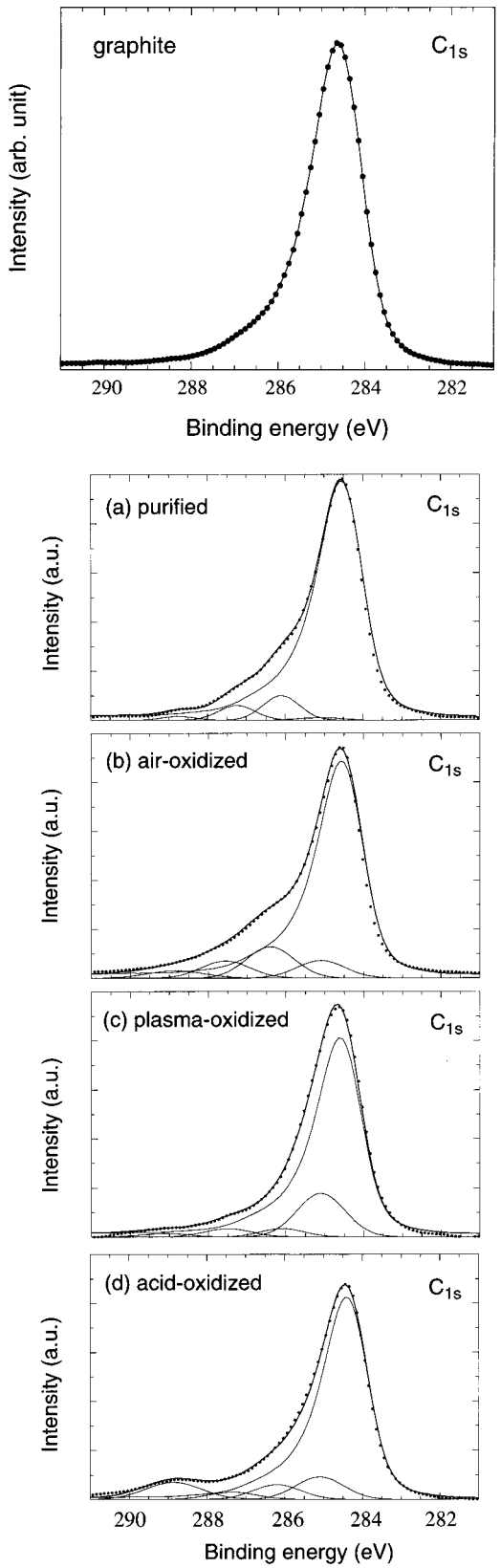

Figure 5. C_{1s} XPS spectra of graphite and (a) purified, (b) air-, (c) plasma-, and (d) acid-oxidized MWNTs. Dots express experimental data points and solid lines are fitting curves for spectra (a)−(d).

positive charge on a carbon atom. Hence, they can be assigned as ⩾C−O− (e.g., alcohol, ether), >C═O (ketone, aldehyde), −COO− (carboxylic acid, ester) species, respectively.

We show the relative intensity for each peak of the C_{1s} spectra in Table 2. The quantitative evaluation of the present curve

TABLE 2: Curve Fitting Results of XPS C_{1s} Spectra

MWNTs	sp2 (%)	sp3 (%)	≻C−O− (%)	>C═O (%)	−COO− (%)	[C(O)]/[C] (%)[a]
purified	90	1	6	3	1	10
air-oxidized	78	5	9	5	3	17
plasma-oxidized	80	14	2	3	1	6
acid-oxidized	79	7	5	2	7	14

[a] Ratio of the carbon atoms which bound to oxygen atoms to all the carbon atoms detected. This is a sum of the three peaks coming from oxidized groups, ≻C−O−, >C═O, and −COO−.

fitting should be treated with care, because (i) we have assumed that the main peak has identical line shape to that of graphite and (ii) the spectra can suffer a contribution from the remaining surfactant. Therefore, we will discuss the results of curve-fitting qualitatively. For purified MWNTs, it is clear that a considerable number of oxygen atoms are bound to the surface carbon atoms. We suspect these oxygen atoms stem from the remaining surfactant as well as oxidized defect sites formed during the purification, particularly the sonication, process. This speculation is consistent with the reduced pπ-nature of purified MWNTs, as compared with graphite observed in the UPS spectra (Figure 3).

Despite the uncertainties in the quantitative analysis, we can see an interesting difference between the oxidized MWNTs (Figure 5(b−d)). For air-oxidized MWNTs, we observed a much higher oxygen concentration than for the purified MWNTs, indicating that not all the oxygen atoms originate from the surfactant. The relative intensity of three peaks which correspond to carbon atoms bound to 1∼3 oxygen atoms is similar to that of the purified MWNTs. It can also be seen that a small portion of sp^3-hybridized carbon atoms are created by the oxidation. For the plasma-oxidized MWNT, we observed greater increase of the sp^3-carbon peak together with a reduction of the main sp^2-carbon peak. We speculate that the application of a strong oxygen plasma caused the destruction of the π-conjugation, followed by transformation to the amorphous carbon phase. This speculation is consistent with the UPS spectrum of the plasma-oxidized MWNTs in which almost no pπ-derived DOS was observed. For acid-oxidized MWNTs, it was confirmed that carboxylic acid groups are preferentially formed by the treatment in the HNO_3/H_2SO_4 mixed solution, in contrast to the other, dry, oxidative treatment. Since no surfactant was used for the acid-oxidized MWNTs, the estimated [O]/[C] ratio should be more reliable than for the other MWNTs. The high concentration of carboxylic acid groups as well as the estimated [O]/[C] ratio of the acid-oxidized MWNT are in good agreement with the previously published work for MWNTs by Hiura et al.[16] We speculate that the observed high work function of the acid-oxidized MWNT stems not only from the high oxygen concentration but also from the acidic carboxylic groups which effectively increase the surface dipole.

We have shown that the gas-phase (air and plasma) and liquid-phase (acid) processes form different oxidized groups on the surface of MWNTs. Surface functional groups on MWNTs after gas-phase oxidation have not been reported so far, as far as we concerned. We have clarified that the gas-phase oxidation leads to the formation of relatively weak acidic groups such as hydroxyl and carbonyl groups. On the other hand, it was observed the acid-oxidation proceeds further to form more acidic carboxylic groups. This liquid-phase oxidation has been widely used because it can control the reaction more easily than the gas-phase oxidation and it proceeds homogeneously over the full length of nanotubes. Recently it has been shown that the liquid-phase oxidation in the presence of sonication shortens SWNTs, resulting in fullerene pipes.[30] It is also interesting to note that the same carboxylic groups were confirmed for acid-oxidized SWNTs by infrared spectra[31] and that the carboxylic acid groups were used as a stage for further chemical modifications.[17] Therefore, the present finding on functional groups formed by gas-phase oxidation provides further possibilities for the modification of carbon nanotubes. The result could also help to design functional nanotubes for each application. For example, we think it is better to treat MWNTs in a gas phase for use as a field emitter because they will have fewer acidic groups, open-tips, and relatively lower work functions.

IV. Conclusions

We have studied photoelectron spectroscopies of purified and oxidized MWNTs in terms of work functions, DOS, and surface functional groups. We determined the work function of purified MWNTs to be 4.3 eV, slightly lower than that of graphite (4.4 eV). The difference is accounted for by the weak binding energy of π-electrons in the MWNTs, possibly as a result of curvature of the graphene layers. In connection with the field emission of MWNTs, it is interesting to study the angle-resolved UPS spectrum to investigate the electron emission from tips of the MWNTs. We found that the electronic structure and the surface chemical species are affected by oxidative treatments. The oxidation of MWNTs by heating in air flow introduces mainly hydroxyl and carbonyl groups and slightly increases the work function (4.4 eV). Plasma treatment destroys the π-conjugation and forms an amorphous carbon phase while increasing the work function up to 4.8 eV. Acid-oxidation preferentially introduces carboxylic acid groups on the surfaces of MWNTs and produced the highest work function (5.1 eV). The increased work functions were explained in terms of a reduction of pπ-derived valence band DOS and the presence of oxygen-induced surface dipole moments. We consider information on the work function to be useful to the design of electronic and/or optoelectronic devices which make use of MWNTs.

Acknowledgment. This work was supported by the Engineering and Physical Sciences Research Council (EPSRC). Raw catalytically grown MWNTs used for acid-oxidation were supplied by Hyperion Catalysts Inc. under contract with A.H.W. Further, H.A. acknowledges the JSPS Research Fellowships for Young Scientists. F.C. acknowledges the Royal Society for the award of University Research Fellowship. We acknowledge K. Tanaka, Y. Ono, and T. Yamabe of Kyoto University and K. Petritsch of Cavendish Laboratory for helpful discussions.

References and Notes

(1) Dresselhaus, M. S.; Dresselhaus, G.; Eklund, P. C. *Science of Fullerenes and Carbon Nanotubes*, Academic Press Inc.: San Diego, 1995.

(2) Tanaka, K.; Yamabe, T.; Fukui, K., Eds. *Science and Technology of Carbon Nanotubes*, Elsevier: Oxford, 1999.

(3) Tanaka, K.; Okahara, K.; Okada, M.; Yamabe, T. *Chem. Phys. Lett.* **1992**, *191*, 469.

(4) Saito, R.; Fujita, M.; Dresselhaus, G.; Dresselhaus, M. S. *Appl. Phys. Lett.* **1992**, *60*, 2204.

(5) Hamada, N.; Sawada, S.; Oshiyama, A. *Phys. Rev. Lett.* **1992**, *68*, 1579.

(6) Mintmire, J. W.; Dunlap, B. I.; White, C. T. *Phys. Rev. Lett.* **1992**, *68*, 631.

(7) Wildöer, J. W. G.; Venema, L. C.; Rinzler, A. G.; Smalley, R. E.; Dekker, C. *Nature* **1998**, *391*, 59.

(8) Odom, T. W.; Huang, J.-L.; Kim, P.; Lieber, C. M. *Nature* **1998**, *391*, 62.

(9) Romero, D. B.; Carrard, M.; de Heer, W. A.; Zuppiroli, L. *Adv. Mater.* **1996**, *8*, 899.

(10) Curran, S. A.; Ajayan, P. M.; Blau, W. J.; Carroll, D. L.; Coleman, J. N.; Dalton, A. B.; Davey, A. P.; Drury, A.; McCarthy, B.; Maier, S.; Strevens, A. *Adv. Mater.* **1998**, *10*, 1091.

(11) Ago, H.; Petritsch, K.; Shaffer, M. S. P.; Windle, A. H.; Friend, R. H. *Adv. Mater.*, in press.

(12) Collins P. G.; Zettl, A. *Phys. Rev. B* **1997**, *55*, 9391.

(13) Tian, M.; Chen, L.; Li, F.; Wang, R.; Mao, Z.; Zhang, Y.; Sekine, H. *J. Appl. Phys.* **1997**, *82*, 3164.

(14) Gulyaev, Y. V.; Sinitsyn, N. I.; Torgashov, G. V.; Mevlyut, S. T.; Zhbanov, A. I.; Zakharchenko, Y. F.; Kosakovskaya, Z. Y.; Chernozatonskii, L. A.; Glukhova, O. E.; Torgashov, I. G. *J. Vac. Sci. Technol. B* **1997**, *15*, 422.

(15) Ebbesen, T. W.; Ajayan, P. M.; Hiura, H.; Tanigaki, K. *Nature* **1994**, *367*, 519.

(16) Hiura, H.; Ebbesen, T. W.; Tanigaki, K. *Adv. Mater.* **1995**, *7*, 275.

(17) Wong, S. S.; Joselevich, E.; Woolley, A. T.; Cheung, C. L.; Lieber, C. M. *Nature* **1998**, *394*, 52.

(18) Shaffer, M. S. P.; Fan, X.; Windle, A. H. *Carbon* **1998**, *36*, 1603.

(19) Rinzler, A. G.; Hafner, J. H.; Nikolaev, P.; Lou, L.; Kim, S. G.; Tománek, D.; Nordlander, P.; Colbert, D. T.; Smalley, R. E. *Science* **1995**, *269*, 1550.

(20) Bonard, J.-M.; Stora, T.; Salvetat, J.-P.; Maier, F.; Stöckli, T.; Duschl, C.; Forró, L.; de Heer, W. A.; Châtelain, A. *Adv. Mater.* **1997**, *9*, 827.

(21) An error of work function determined from cutoff of the secondary electron of UPS HeI spectra is, generally, 0.1 eV. Although the difference of work functions of the purified MWNT film and graphite is within this error, we believe the relative difference measured with the identical setup represents intrinsic properties. For example, we have obtained the same relative difference (0.1 eV) for the work functions of the purified and air-oxidized MWNT films, but their UPS and XPS spectra showed clear difference (Figures 3 and 5).

(22) Biaconi, A.; Hagström, S. B. M.; Bachrach, R. Z. *Phys. Rev. B* **1977**, *16*, 5543.

(23) Kuzuo, R.; Terauchi, M.; Tanaka, M. *Jpn. J. Appl. Phys.* **1992**, *31*, L1484.

(24) Ago, H.; Keil, M.; Kugler, T.; Cacialli, F.; Tsukagoshi, K.; Friend, R. H.; Salaneck, W. R., in preparation.

(25) Ajayan, P. M.; Ebbesen, T. W.; Ichihashi, T.; Iijima, S.; Tanigaki, K.; Hiura, H. *Nature* **1993**, *362*, 522.

(26) Atamny, F.; Blöcker, J.; Dübotzky, A.; Kurt, H.; Timpe, O.; Loose, G.; Mahdi, W.; Schlögl, R. *Mol. Phys.* **1992**, *76*, 851.

(27) Mansour, A.; Ugolini, D. *Phys. Rev. B* **1993**, *47*, 10201.

(28) Th, P. M.; Attekum, M.; Wetheim, G. K.; *Phys. Rev. Lett.* **1979**, *43*, 1896.

(29) Díaz, J.; Paolicelli, G.; Ferrer, S.; Comin, F. *Phys. Rev. B* **1996**, *54*, 8064.

(30) Liu, J.; Rinzler, A. G.; Dai, H.; Hafner, J. H.; Bradley, R. K.; Boul, P. J.; Lu, A.; Iverson, T.; Shelimov, K.; Huffman, C. B.; Macias, F. R.; Shon, Y. S.; Lee, T. R.; Colbert, D. T.; Smalley, R. E. *Science* **1998**, *280*, 1253.

(31) Chen, J.; Hamon, M. A.; Hu, H.; Chen, Y.; Rao, A. M.; Eklund, P. C.; Haddon, R. C. *Science* **1998**, *282*, 95.